OPEN

Citation: Transl Psychiatry (2015) 5, e496; doi:10.1038/tp.2014.128

www.nature.com/tp

ORIGINAL ARTICLE

Aggrecan and chondroitin-6-sulfate abnormalities in schizophrenia and bipolar disorder: a postmortem study on the amygdala

H Pantazopoulos[1,2], M Markota[1,2], F Jaquet[1], D Ghosh[1], A Wallin[1], A Santos[1], B Caterson[3] and S Berretta[1,2,4]

Perineuronal nets (PNNs) are specialized extracellular matrix aggregates surrounding distinct neuronal populations and regulating synaptic functions and plasticity. Previous findings showed robust PNN decreases in amygdala, entorhinal cortex and prefrontal cortex of subjects with schizophrenia (SZ), but not bipolar disorder (BD). These studies were carried out using a chondroitin sulfate proteoglycan (CSPG) lectin marker. Here, we tested the hypothesis that the CSPG aggrecan, and 6-sulfated chondroitin sulfate (CS-6) chains highly represented in aggrecan, may contribute to these abnormalities. Antibodies against aggrecan and CS-6 (3B3 and CS56) were used in the amygdala of healthy control, SZ and BD subjects. In controls, aggrecan immunoreactivity (IR) was observed in PNNs and glial cells. Antibody 3B3, but not CS56, also labeled PNNs in the amygdala. In addition, dense clusters of CS56 and 3B3 IR encompassed CS56- and 3B3-IR glia, respectively. In SZ, numbers of aggrecan- and 3B3-IR PNNs were decreased, together with marked reductions of aggrecan-IR glial cells and CS-6 (3B3 and CS56)-IR 'clusters'. In BD, numbers of 3B3-IR PNNs and CS56-IR clusters were reduced. Our findings show disruption of multiple PNN populations in the amygdala of SZ and, more modestly, BD. Decreases of aggrecan-IR glia and CS-6-IR glial 'clusters', in sharp contrast to increases of CSPG/lectin-positive glia previously observed, indicate that CSPG abnormalities may affect distinct glial cell populations and suggest a potential mechanism for PNN decreases. Together, these abnormalities may contribute to a destabilization of synaptic connectivity and regulation of neuronal functions in the amygdala of subjects with major psychoses.

Translational Psychiatry (2015) **5,** e496; doi:10.1038/tp.2014.128; published online 20 January 2015

INTRODUCTION

Chondroitin sulfate proteoglycans (CSPGs) are one of the main components of the brain extracellular matrix (ECM). Emerging evidence from human postmortem, animal model and genetic studies points to their involvement in the pathophysiology of schizophrenia (SZ).[1–7] Postmortem studies show abnormalities of CSPG-enriched perineuronal nets (PNNs), specialized ECM aggregates enveloping distinct neuronal populations, in subjects with SZ. Specifically, PNNs labeled with a lectin CSPG marker, that is, *Wisteria floribunda* agglutinin (WFA), are decreased in the amygdala, entorhinal cortex and prefrontal cortex, but not visual cortex, of subjects with this disorder.[3,4] In the amygdala and entorhinal cortex, WFA-positive PNN decreases were accompanied by sharp, widespread, increases of WFA-positive glial cells.[3] Together with reduced CSPG expression in the olfactory epithelium,[1] these findings suggest that CSPG abnormalities may be region-selective but inclusive of a wide range of neural structures in SZ. Rodent studies are consistent with a role of PNNs in SZ. Models of oxidative stress relevant to this disorder show reductions of PNNs,[8] whereas localized PNN destruction reproduces functional abnormalities reminiscent of SZ.[9] Finally, polymorphisms of genes encoding for several CSPGs have been associated with SZ.[5–7]

ECM/CSPG functions resonate with key pathophysiological aspects of SZ, such as anomalies affecting neuronal migration, neural connectivity, synapses, glia, glutamatergic transmission and inhibitory intrinsic circuitry.[2,10–26] During development, the ECM, and CSPGs in particular, regulate neuronal migration, axon outgrowth, synaptogenesis and synaptic maturation.[23,27–31] CSPG-enriched PNNs form in an activity-dependent manner during late postnatal development, completing neuronal maturation.[32–34] This process is critically dependent on glial cells, which secrete and organize CSPGs and other ECM molecules.[35–37] Once formed, and throughout adulthood, PNNs control neuronal access to growth and transcription factors, stabilize synaptic connectivity and compartmentalize the neuronal surface, regulating the availability of glutamatergic receptors to postsynaptic specializations and, thus, neuronal firing properties.[23,25,38] Among several neuronal populations enveloped by PNNs, GABAergic interneurons are one of the largest and most extensively investigated.[39–41] The function and plasticity of these neurons is thus intrinsically linked to their association with PNNs. Together, these considerations raise the possibility that CSPG abnormalities in SZ may contribute to, and potentially represent a unifying factor for, key aspects of the pathophysiology of this disorder.

Because they serve specialized roles during brain development and adulthood, it is crucial to assess which specific CSPGs are altered in SZ. CSPGs are composed of specific core proteins to which chondroitin sulfate (CS) chains are attached[42] (Figure 1). Numbers of CS chains and their patterns of sulfation fundamentally affect their functions, such as their ability to interact with

[1]Translational Neuroscience Laboratory, Mclean Hospital, Belmont, MA, USA; [2]Department of Psychiatry, Harvard Medical School, Boston, MA, USA; [3]School of Biosciences, Cardiff University, Cardiff, UK and [4]Program in Neuroscience, Harvard Medical School, Boston, MA, USA. Correspondence: Dr S Berretta, MRC3 McLean Hospital—Mailstop 149, 115 Mill Street, Belmont, MA 02478, USA.
E-mail: s.berretta@mclean.harvard.edu
Received 21 July 2014; revised 8 October 2014; accepted 26 October 2014

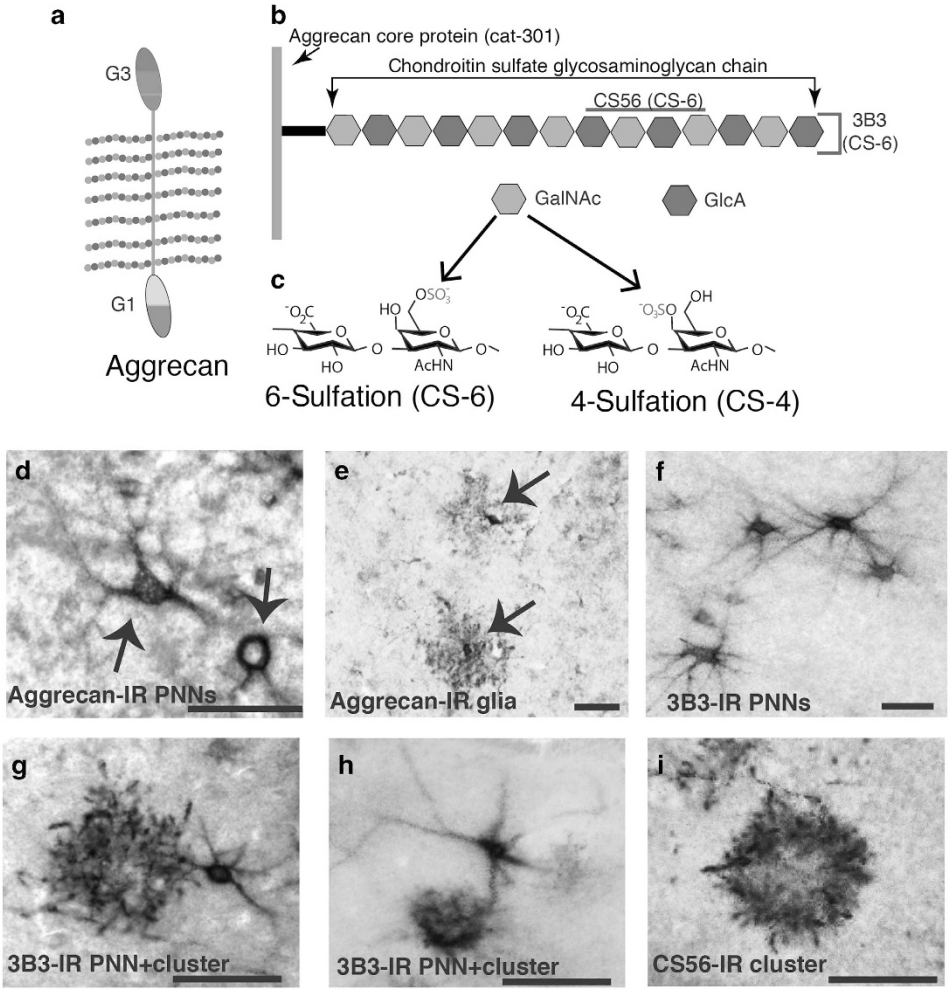

Figure 1. CSPG structure and aggrecan and CS-6 labeling in the normal human amygdala. Chondroitin sulfate proteoglycans (CSPGs) are composed of core proteins with covalently attached chondroitin sulfate (CS) glycosaminoglycan chains. (**a**) A schematic representation of aggrecan, with its core protein and polysaccharide chains, shown in more detail in (**b**). These chains consist of pairs of glucuronic acid (GlcA) and *N*-acetyl-galactosamine (GalNAc). This latter can be sulfated in position 6 (CS-6) or 4 (CS-4) (**c**). The antibody 3B3 detects a non-reducing terminal end saturated CS disaccharide consisting of glucuronic acid *N*-acetyl-galactosamine-6-sulfate (CS-6).[50,51] The antibody CS56 detects an A–D sequence in reducing octasaccharide units on both CS-C (CS-6) and CS-D (CS-2,6) chondroitin sulfate.[52,53] Photomicrographs in (**d**–**i**) depict immunolabeling with 3B3, CS56 and antibodies raised against aggrecan. Aggrecan-IR PNNs (**d**) and aggrecan-IR glial cells (**e**), detected with the antibody cat-301 in the amygdala of a control subject. Shown in (**f**–**h**) are 3B3-IR PNNs and glial clusters, respectively. 3B3-IR PNNs were often found in close contact with 3B3-IR glial cluster. Antibody CS56 labeled exclusively glial clusters (**i**). Scale bar, 50 μm. IR, immunoreactivity; PNN, perineuronal net.

other molecules including growth factors and cytokines.[43] Chondroitin-4-sulfation (CS-4) and chondroitin-6 sulfation (CS-6) are the two most common sulfation patterns in the brain, with several variations depending on the position of the sulfation on the CS chains[43,44] (Figure 1). For the present investigations, we focused on the CSPG aggrecan and the CS-6 sulfation pattern. Aggrecan is a major component of the brain ECM and of at least a subgroup of PNNs, and contains numerous CS chains with a predominant CS-6 representation.[45,46] In parallel to PNN development, aggrecan expression coincides with the maturation of electrophysiological properties of neurons and the formation of synapses during late stage developmental periods.[47,48] Furthermore, aggrecan and CS-6 expression in glial cells are involved in the regulation of astrocyte maturation, which, in turn, has a key role in PNN formation and maintenance.[35,49] With the present postmortem study, we tested the hypothesis that aggrecan and CS-6 patterns contribute to PNN and glia abnormalities in SZ. Subjects with bipolar disorder (BD) were included in these investigations to assess whether these abnormalities are specific to SZ or instead shared across major psychotic disorders.

MATERIALS AND METHODS

Human subjects

Tissue blocks containing the whole amygdala from a cohort of normal control donors ($n = 29$), and donors with SZ ($n = 24$) or BD ($n = 20$) and were used for histochemical and immunocytochemical investigations (Supplementary Tables 1–3). A sub-cohort of these subjects, that is, normal control ($n = 12$), SZ ($n = 12$) and bipolar disorder ($n = 13$) donors, was used for the aggrecan study. This sub-cohort overlapped to a great extent to the one used for the WFA study previously published,[3] that is, 12 out of 12 controls, 10 out of 12 subjects with SZ and 9 out of 13 subjects with BD were included in both studies. The sub-cohorts included in the CS56 (control, $n = 13$; SZ, $n = 14$; BD, $n = 8$) and 3B3 (control, $n = 14$; SZ, $n = 13$; BD, $n = 8$) studies largely overlap with each other, but only minimally with that used for aggrecan and WFA (Supplementary Tables 1–3). Additional tissue blocks from 14 normal controls and 14 SZ subjects were used for quantitative PCR with reverse transcription (Supplementary Materials; Supplementary Tables 2–3). All tissue blocks were obtained from

the Harvard Brain Tissue Resource Center (HBTRC), McLean Hospital, Belmont, MA, USA. Diagnoses of SZ and BD were made by two psychiatrists on the basis of retrospective review of medical records and extensive questionnaires concerning social and medical history provided by the family members. Several regions from each brain were examined by a neuropathologist. The cohort used for this study did not include subjects with evidence for gross and/or macroscopic brain changes, or clinical history consistent with cerebrovascular accident or other neurological disorders. Subjects with Braak stages III or higher (modified Bielchowsky stain) were not included. None of the subjects had significant history of substance dependence within 10 or more years from death, as further corroborated by negative toxicology reports. Absence of recent substance abuse is typical for samples from the HBTRC, which receives exclusively community-based tissue donations.

Tissue processing

Tissue blocks for immunohistochemistry were dissected from fresh brains and post-fixed in 0.1 M phosphate buffer containing 4% paraformaldehyde and 0.1 M Na azide at 4 °C for 3 weeks, then cryoprotected at 4 °C for 3 weeks (30% glycerol, 30% ethylene glycol and 0.1% Na azide in 0.1 M phosphate buffer), embedded in agar and pre-sliced in 2 mm coronal slabs using an Antithetic Tissue Slicer (Stereological Research Lab, Aarhus, Denmark). Each slab was exhaustively sectioned using a freezing microtome (American Optical 860, Buffalo, NY, USA). Sections were stored in cryoprotectant at − 20 °C. Using systematic random sampling criteria, sections through the amygdala were serially distributed in 26 compartments (40 μm thick sections; 10–12 sections per compartment; 1.04-mm section separation within each compartment). All sections within one compartment per subject were selected for each marker (that is, cat-301, 3B3, CS56), thus respecting the 'equal opportunity' rule.[54,55] Tissue blocks for RNA analysis were dissected from fresh brains and quickly frozen in liquid nitrogen vapor. Ten-micrometer thick sections were cut on a cryostat, dissected into distinct amygdala nuclei and placed into miRVana RNA lysis/binding buffer for RNA extraction.

Primary antibodies—histological markers

Aggrecan (cat-301): Cat-301 (MAB5284, lot# LV1353393, Chemicon International, Temecula, CA, USA) is a monoclonal antibody raised against feline spinal cord gray matter. This antibody recognizes a distinct glycosylated form of the aggrecan core protein in human and primate brain tissue,[56,57] and was chosen over other antibodies raised against aggrecan, such as cat-315 and cat-316, which detect oligosaccharides on the aggrecan CS chains instead.[56]

CS56: CS56 is a mouse monoclonal IgM (Sigma-Aldrich, St Louis, MO, USA; C8035, lot# 056K4804) made using vertebral membranes from chicken gizzard fibroblasts as an immunogen. The CS structure immunoreactive for CS56 has been identified as an A–D sequence in reducing octosaccharide units on both CS-C (CS-6) and CS-D (CS-2,6) chondroitin sulfate.[52,53] CS56 has been reported to specifically label CS-6 in brain tissue.[43] CS56 immunolabeling is virtually absent in CS6ST-1-deficient mice that do not produce CS-6 (personal communication, Dr Hiroshi Kitagawa, PhD, Kobe Pharmaceutical University).

3B3: 3B3 is a mouse monoclonal antibody developed by Dr Bruce Caterson, PhD. If used without pre-incubation with chondroitinase ABC, as in this study, it detects a saturated CS glycosaminoglycan disaccharide consisting of a non-reducing glucuronic acid *N*-acetyl-galactosamine-6-sulfate (CS-6) on the terminal end of CS chains.[50,51]

GFAP: Rabbit polyclonal anti-GFAP was generated using full-length recombinant human GFAP (Abcam ab7260, lot# GR20948-7). Western blot assay shows that this antibody detects a 55 kDA band in western blots corresponding to GFAP (Abcam, Cambridge, MA, USA).

Wisteria floribunda agglutinin: WFA, a lectin isolated from the seeds of *Wisteria floribunda*, binds specifically to *N*-acetyl-D-galactosamine on the terminal end of CS chains, with a preference for beta glycosidic linkage.[58] The specificity of WFA as a marker for these macromolecules is supported by extensive literature, including ablation of labeling following CS enzymatic digestion.[3,59–61]

Immunocytochemistry

Antigen retrieval was carried out by placing free-floating sections in citric acid buffer (0.1 M citric acid, 0.2 M Na_2HPO_4) heated to 80 °C for 30 min. Sections were then incubated in primary antibody (cat-301, 2 :1000 μl; CS56, 0.25:1000 μl; 3B3, 10:1000 μl) for 48–72 h at 4 °C, and then in biotinylated secondary serum (cat-301, horse anti-mouse IgG; 3B3 and CS56 goat anti-mouse IgM; 1: 500 μl; Vector Labs, Burlingame, CA, USA). This step was followed by streptavidin conjugated with horse-radish peroxidase for 2 h (1:5000 μl, Zymed, San Francisco, CA, USA) and, finally, nickel-enhanced diaminobenzidine/peroxidase reaction (0.02% diaminobenzidine, Sigma-Aldrich, 0.08% nickel-sulfate, 0.006% hydrogen peroxide in phosphate buffer). All solutions were made in phosphate-buffered saline with 0.5% Triton X unless otherwise specified.

All sections were mounted on gelatin-coated glass slides, coverslipped and coded for quantitative analysis blinded to diagnosis. Sections from all the brains included in the study were processed simultaneously within the same session to avoid procedural differences. Each six-well staining dish contained sections from SZ, BD and normal control subjects and was carried through each step for the same duration of time, so as to avoid sequence effects. Omission of the first (cat-301, 3B3 or CS56) or secondary antibodies did not result in detectable signal.

Quantitative PCR with reverse transcription

Frozen tissue samples were processed for total RNA isolation and purification and transcript variants 1 and 2 of the human aggrecan gene (ACAN) were detected by quantitative PCR with reverse transcription using the Taqman gene expression assay Hs00153936_m1 and GAPDH, RPII and HPRT1 as reference genes. Normalization of aggrecan gene expression to GAPDH, RPII and HPRT1 gene expression and comparison of gene expression between diagnosis groups was calculated according to the $2^{-\Delta\Delta Ct}$ method by Livak and Schmittgen[62,63] (for more details, see Supplementary Materials).

Data collection

A Zeiss Axioskop 2 Plus interfaced with StereoInvestigator 6.0 (Microbrightfield, Willinston, VT, USA) was used for the analysis. The borders of the lateral (LN), basal (BN), accessory basal (AB), cortical (CO), medial (ME) and central (CE) nuclei of the amygdala (Figure 2) were identified according to cytoarchitectonic criteria as described by Sims and Williams[64] and Amaral *et al.*[65] The nomenclature adopted was that used by Sorvari *et al.*[66] The intercalated cell masses were not included within the borders of these nuclei. The paralaminar nucleus could not be distinguished reliably from the ventral basal nucleus and was thus included within its borders. A ×1.6 objective was used to trace the borders of amygdalar nuclei. Each traced region was systematically scanned through the full x, y and z axes using a ×40 objective to count each immunoreactive (IR) element within the traced borders over complete sets of serial sections (6–10 sections) representing the whole extent of the amygdala from each subject, with a section interval of 1040 μm. This method has the advantage of minimizing the risk of errors in estimating poorly represented and/or unevenly distributed elements, such as those investigated in this study.[41,67]

Numerical densities and total numbers estimates. Numerical densities (Nd) were calculated as $Nd = \Sigma N / \Sigma V$, where N is the sum of cells within a region of interest, and V is the total volume of the region of interest. Total number (Tn) of IR elements (PNNs, glia, glial cell clusters) was calculated as $N = i \times \Sigma n$ where Σn = sum of the cells counted in each subject, and i is the section interval (that is, number of serial sections between each section and the next within each compartment = 26), as described previously in detail.[68]

Statistical analysis

Differences between groups relative to the main outcome measures in each of the regions examined were assessed for statistical significance using an analysis of covariance stepwise linear regression process. Effect sizes were calculated according to Hedges' g. A logarithmic transformation was uniformly applied to all original values because the data were not normally distributed. Statistical analyses were performed using JMP v5.0.1a (SAS Institute, Cary, NC, USA). BD and SZ were compared separately with normal controls. Age, gender, postmortem time interval, inflammation (classified as positive or negative for inflammatory condition at the time of death), hemisphere, cause of death, brain weight, exposure to alcohol, nicotine, electroconvulsive therapy, and lifetime, as well as final 6 months', exposure to antipsychotic drugs, exposure to selective serotonin reuptake inhibitors classified as positive or negative for exposure, and lithium treatment were tested systematically for their effects on the main outcome measures, and included in the model if they significantly improved the model goodness of fit. Values relative to the *t* ratio and *P*-value for main

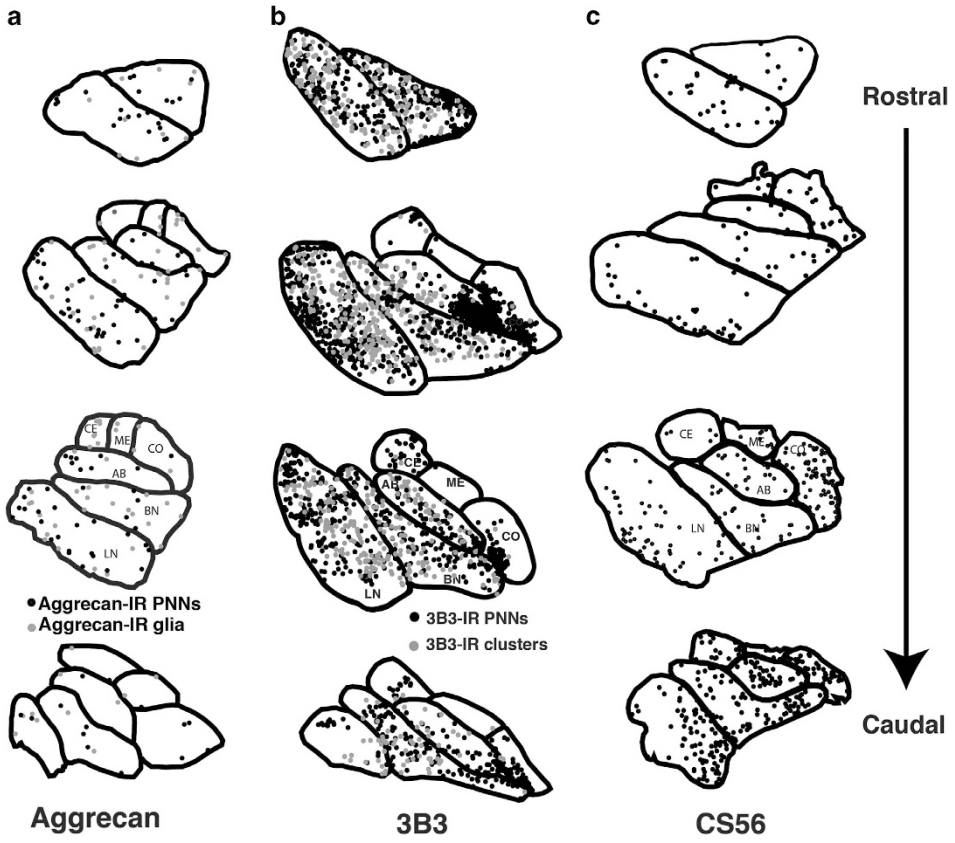

Figure 2. Distribution of aggrecan, 3B3 and CS56-IR PNN (black dots) and glia/glial clusters (gray dots) in the normal human amygdala. (**a**) Aggrecan-IR PNNs and glial cells were located mainly in the lateral (LN) and basal (BN) nuclei of the amygdala, whereas smaller numbers were observed in the accessory basal (AB), cortical (CO), medial (ME) and central (CE) nuclei. 3B3-IR PNNs and glial cell clusters (**b**) were more numerous than aggrecan or CS56-IR elements, but similarly distributed across the amygdala nuclei. CS56-IR was observed only in glial clusters (**c**), broadly distributed across the amygdala nuclei, and less numerous than 3B3-IR glial clusters. CS, chondroitin sulfate; IR, immunoreactivity; PNN, perineuronal net.

outcome measure differences found to be statistically significant are reported in Supplementary Tables 4–6. Any and all covariates found to affect an outcome measure significantly are also reported.

Cause of death was categorized as acute (for example, myocardial infarction) or chronic (for example, cancer). Data on nicotine and alcohol exposure were only available for subjects with SZ or BD; on the basis of the subjects' record, exposure was considered as high, moderate, low and absent, as well as present or absent during the last 10 years of life. We analyzed the medical records for exposure to various classes of psychotropic and neurotropic drugs. Estimated daily mg doses of antipsychotic drugs were converted to the approximate equivalent of chlorpromazine as a standard comparator,[69] and corrected on the basis of a qualitative assessment of treatment-adherence based on taking prescribed psychotropic medicines more or less than approximately half of the time, as indicated by the extensive antemortem clinical records. These values are reported as lifetime, as well as last 6 months' of life, grams per patient (Supplementary Table 3). Exposure to lithium salt was estimated in the same manner (Supplementary Table 3). Exposure to other classes of psychotropic drugs was reported as present or absent (Supplementary Table 3). These variables, as well as subtypes of SZ (for example, paranoid, catatonic, disorganized) and measures of life quality (for example, dependent/independent), could not be tested reliably because the number of subjects in each category was too low. However, these variables were taken into account as a possible explanation when apparent clustering of subjects was observed. In addition to testing the potential effects of exposure to antipsychotics and lithium salt within our stepwise linear regression process, the effects of these variables, together with other psychotropic and neurotropic drugs, adherence to pharmacological treatment (good or poor), age of onset of the disease and duration of the illness, were tested directly in separate analyses of variance.

RESULTS

Aggrecan and CS-6 expression in the normal human amygdala

PNN. Aggrecan IR was observed in PNNs predominantly located within the LN. A large number of 3B3-IR PNNs were detected throughout the amygdala, outnumbering by far aggrecan-IR PNNs (Supplementary Tables 4 and 5) as well as WFA-positive PNNs,[3,67] particularly within the BN, ABN, CO and CE/ME (Supplementary Tables 4 and 5). Within the LN, approximately half (54%) of the aggrecan-IR PNNs and over 80% of the 3B3-IR PNNs are also labeled with WFA (see Supplementary Materials for details). CS56 did not label PNNs.

Glia. A small number of aggrecan-IR glia were scattered in all the amygdala nuclei examined. These cells were not labeled by WFA and did not show GFAP-IR (see also Supplementary Materials). Numerous clusters of dense CS56- and 3B3-IR product, encompassing CS56- and 3B3-IR cells, respectively, morphologically identifiable as glia and showing faint GFAP-IR, were detected in all the amygdala nuclei examined (Figures 1 and 3). WFA labeling was not detected in these clusters. We refer to these structures, that is, CS-6-IR glia surrounded by diffuse CS-6-IR, as 'glial clusters'. Quantitative analysis for normal and comparison studies (below) focused on the number of glial clusters because under light microscopy the intensity of the diffuse immunolabeling did not allow clear identification of individual CS-6-IR glial cells (Figures 1g-i), and the large majority of these cells are contained within the clusters. We estimate that each glial cluster may contain approximately two to seven CS-6-IR glial cells. Notably, several 3B3-IR PNNs were observed in close contact with 3B3-IR glial

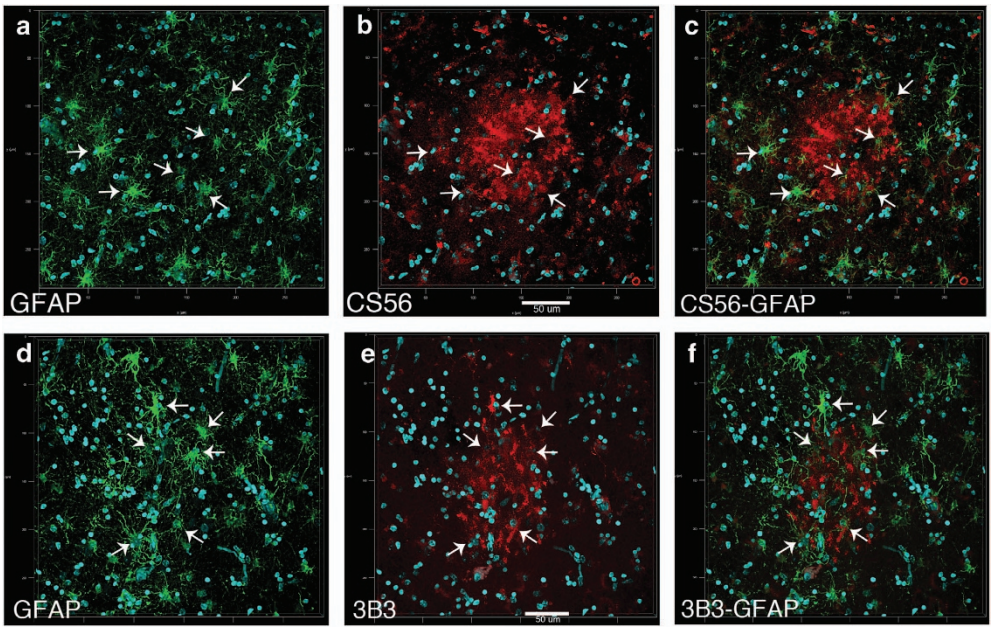

Figure 3. CS-6-IR glial clusters contain GFAP-IR astrocytes. Dual-immunofluorescence confocal microscopy was used to investigate the relationship between CS-6 glial clusters and GFAP-IR astrocytes. (**a**–**c**) GFAP-IR cells are shown within, and surrounding, CS56-IR clusters. A large number of these GFAP-IR cells also show CS56-IR (arrows indicate the location of GFAP/CS56-IR cells within the CS56-IR cluster). Although CS56 IR was often only faintly detected in GFAP-IR cell bodies, evidence from rodent studies suggests more intense CS56-IR in the terminal ends of their processes within the clusters.[70] Glial clusters immunolabeled with 3B3 showed a similar relationship to GFAP-IR glial cells ((**d**–**f**); arrows indicate the location of GFAP/3B3-IR cells within the 3B3-IR cluster). Scale bar, 50 μm. CS, chondroitin sulfate; IR, immunoreactivity; PNN, perineuronal net.

clusters (Figures 1g and h), suggesting functional relationships between the two elements.

Decrease of aggrecan-IR PNNs and glia, but increased aggrecan mRNA expression, in schizophrenia

In subjects with SZ, Tn and Nd of aggrecan-IR PNNs were significantly decreased in the LN (Tn, $P<0.03$, $g=-0.95$; Dn, $P<0.04$, $g=-0.93$; adjusted for cause of death, $P<0.003$; Figure 4, Supplementary Table 4). Aggrecan-IR glia (Tn) were significantly decreased in the LN ($P<0.01$, $g=-1.11$), BN ($P<0.01$, $g=-1.19$) and ABN ($P<0.005$, $g=-1.28$); significance values adjusted for the effects of PMI ($P=0.01$; Figure 4, Supplementary Table 4). Aggrecan mRNA expression was significantly increased in the LN of SZ subjects ($P<0.03$; $g=0.90$; see Supplementary Figure 3).

In subjects with BD, aggrecan-IR PNNs (Tn, but not Nd) were decreased in the LN ($P<0.04$, $g=-0.88$; Figure 4, Supplementary Table 4). Tn and Nd of aggrecan-IR PNNs were decreased in the ABN (Tn, $P<0.04$, $g=-0.92$; Dn, $P<0.03$, $g=-1.37$; corrected for lifetime exposure to lithium, $P<0.01$; Figure 4, Supplementary Table 4). No changes in aggrecan-IR glia were observed in BD (Figure 4, Supplementary Table 4).

Decreased 3B3-IR PNNs and glial clusters in schizophrenia and bipolar disorder

In subjects with SZ, 3B3-IR PNNs were decreased in the LN (Tn, $P<0.01$, $g=-1.37$; Dn, $P<0.03$, $g=-0.87$), BN (Tn, $P<0.002$, $g=-2.12$; Nd, $P<0.006$, $g=-1.49$), ABN (Tn, $P<0.002$, $g=-1.68$; Nd, $P<0.009$, $g=-1.44$), CO (Tn, $P<0.001$, $g=-1.88$; Nd, $P<0.003$, $g=-1.65$), and ME (Tn, $P<0.04$, $g=-1.04$). In the CE, 3B3-IR PNN decreases did not reach statistical significance, although the effect sizes were very large (Tn, $P<0.06$, $g=-0.91$; Nd, $P=0.07$, $g=-1.02$; Figure 5, Supplementary Table 5). Significance values for each nucleus were adjusted for the effects of cause of death ($P<0.03$), PMI ($P<0.15$), included *a priori* due to its significant positive effect on PNN Tn and Nd in SZs ($P<0.01$), and VPA ($P<0.03$). Decreases were also observed for 3B3-IR glial clusters in LN (Tn, $P<0.0003$, $g=-1.93$; Nd, $P<0.0007$, $g=-1.74$), BN (Tn, $P<0.0006$, $g=-1.77$; Nd, $P<0.002$, $g=-1.53$), ABN (Tn, $P<0.001$, $g=-1.63$, Nd, $P<0.005$, $g=-1.40$), CO (Tn, $P<0.02$, $g=-1.12$; Nd, $P<0.04$, $g=-0.95$), CE (Tn, $P<0.03$, $g=-0.98$; Nd, $P=0.06$, $g=-0.9$) and ME (Tn, $P<0.005$, $g=-1.36$; Nd, $P<0.03$, $g=-1.09$). Significance values for each nucleus were adjusted for effects of age ($P<0.001$) and cause of death ($P<0.002$; Figure 5, Supplementary Table 5).

In subjects with BD, 3B3-IR PNNs were decreased in the LN (Tn, $P<0.002$, $g=-2.14$; Nd, $P<0.002$, $g=-2.00$), BN (Tn, $P<0.01$, $g=-1.01$; Nd, $P<0.005$, $g=-1.93$), AB (Tn, $P<0.05$, $g=-0.94$; Nd, $P<0.004$, $g=-1.97$) and ME (Tn, $P<0.007$, $g=-2.16$; Nd, $P<0.03$, $g=-1.32$). Significance values for each nucleus were adjusted for effects of lifetime lithium ($P<0.05$; Figure 5, Supplementary Table 5). Decreases in 3B3-IR glial clusters were observed only in the ME (Tn, $P<0.03$, $g=-1.05$; Figure 5, Supplementary Table 5).

Decreased CS-6 (CS56) glial clusters in schizophrenia and bipolar disorder

In subjects with SZ, CS56-IR glial clusters were significantly decreased in the LN (Tn, $P<0.0004$, $g=-2.09$; Nd, $P<0.002$, $g=-1.80$), BN (Tn, $P<0.0005$, $g=-2.00$; Nd, $P<0.002$, $g=-1.74$), ABN ($P<0.01$, $g=-1.39$; Nd, $P<0.02$, $g=-1.21$), CE (Tn, $P<0.007$, $g=-1.64$; Nd, $P=0.04$, $g=-1.17$) and ME (Tn, $P<0.04$, $g=-1.08$; Nd, $P<0.06$, $g=-0.98$; Figure 5, Supplementary Table 6). Decreases in the CO did not reach statistical significance, although the effect size was relatively large (Tn, $P<0.06$, $g=-0.98$; Nd, $P<0.06$, $g=-0.95$). Significance values were adjusted for exposure to selective serotonin reuptake inhibitors (SSRIs; $P<0.05$), which showed positive correlations with CS56-IR clusters.

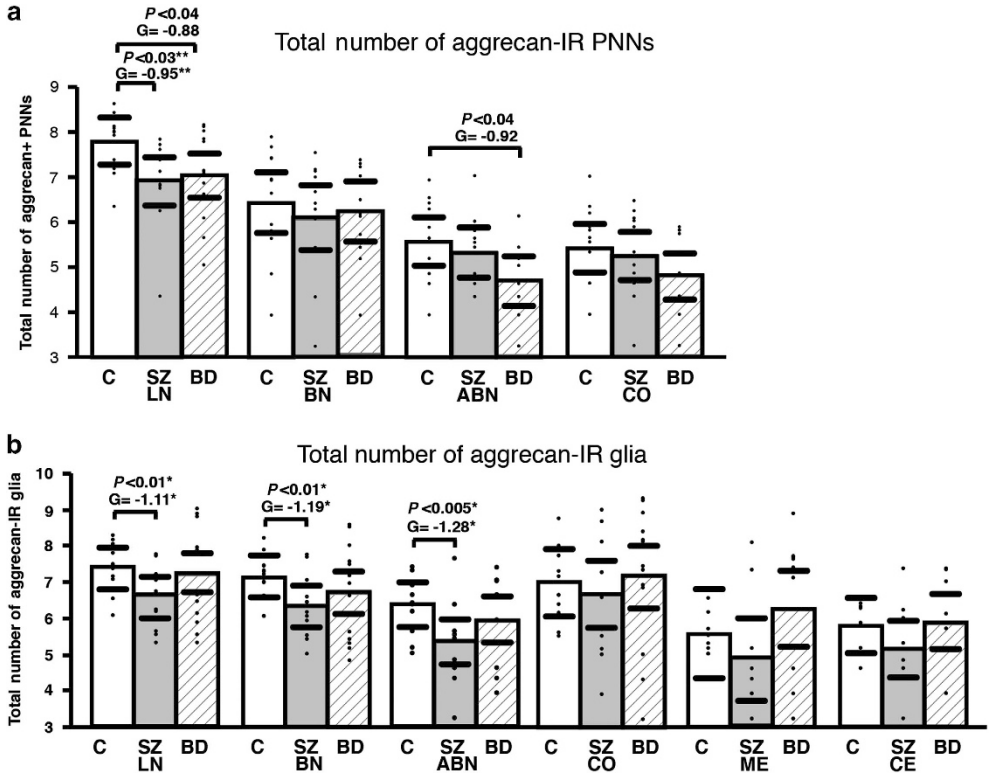

Figure 4. Aggrecan-IR PNN and glial cell are decreased in the amygdala of subjects with SZ. Total numbers of aggrecan-IR PNNs were significantly decreased in the LN of SZ and BD subjects, and in the AB of BD subjects (**a**). Total numbers aggrecan-IR glia were significantly decreased in the LN, BN, AB of SZ subjects (**b**). A decrease in the CE was only significant for numerical densities (Supplementary Table 4). No changes were observed in BD subjects. Significance values are derived from stepwise linear regression models. Scatterplots show the mean (histogram) and 95% confidence intervals (black lines). *Adjusted for effect of PMI. **Adjusted for effect of cause of death. ABN, accessory basal nucleus; BD, bipolar disorder; BN, basal nucleus; CE, central nucleus; CO, cortical nucleus; IR, immunoreactivity; LN, lateral nucleus; ME, medial nucleus; PNN, perineuronal net; SZ, schizophrenia.

In BD subjects, significant decreases of CS56-IR glial clusters were observed in the LN (Tn, $P < 0.002$, $g = -2.52$; Nd, $P = 0.0005$, $g = -2.90$), BN (Tn, $P < 0.0006$, $g = -2.19$; Nd, $P < 0.003$, $g = -2.33$), ABN (Tn, $P < 0.009$, $g = -1.98$; Nd, $P < 0.004$, $g = -2.22$), and CE (Tn, $P < 0.04$, $g = -1.53$; Nd, $P < 0.006$, $g = -2.11$; Figure 5, Supplementary Table 6). Significance values were adjusted for lithium exposure (lifetime; $P < 0.05$), which showed a positive correlation with CS56-IR clusters.

DISCUSSION

Our results point to marked abnormalities in the expression of aggrecan and CS-6 in subjects with SZ and subjects with BD (Table 1). In particular, aggrecan-IR PNNs and glia were decreased in SZ, whereas only modest aggrecan-IR PNN decreases were present in BD. Numbers of CS-6 IR glial clusters and PNNs were markedly reduced in SZ and BD. Changes in BD provide the first evidence for anomalies of PNNs and CSPG expression in this disorder, and point to partially overlapping abnormalities of these elements in SZ and BD. PNN reductions affect neuronal populations larger than previously demonstrated, encompassing several amygdala nuclei,[3] and suggest altered neuronal maturation and firing properties and instability of neuronal synaptic connectivity. In sharp contrast to increases of WFA-positive glial cells reported previously in SZ,[3] aggrecan-IR glia and CS-6- (3B3 and CS56)-IR glial clusters were markedly decreased. We suggest that decreases of CSPG-positive glial cells may provide important clues on the potential mechanisms of PNN abnormalities, raising the possibility that distinct glial cell populations may fail to synthesize and secrete key CSPGs required to maintain PNN integrity.

Technical considerations

Pharmacological treatment and drugs of abuse. Effects of pharmacological treatment detected in these studies were limited to SSRIs and lithium on a small number of outcome variables (Supplementary Tables 4–6). These effects are consistent with a corrective mechanism, showing positive correlations with CSPG-IR PNNs and glia in the face of significant decreases of these elements in diagnosis groups. SSRI exposure in SZ subjects was significantly and positively correlated with Tn and Nd of CS56-IR glial cell clusters (Supplementary Table 6). Records for SSRI exposure in BD subjects were insufficient to assess these effects. Lithium exposure correlated positively with CS56-IR glia in subjects with BD. This effect was somewhat unexpected because lithium treatment was shown in rodents to facilitate enzymatic CSPG digestion.[71,72] It is possible that chronic exposure to lithium treatment in BD, species differences, and perhaps the interaction of lithium with altered CSPG biochemistry in BD may account for this effect.

The subjects included in this study had no significant history of substance dependence within 10 or more years from death. Lack of recent exposure was further corroborated by negative toxicology reports provided by the HBTRC. In addition, no significant effects were observed with ethanol or nicotine exposure on any of the outcome measures tested.

CSPG labeling. In this study, aggrecan was detected using the antibody cat-301, widely used in investigations on PNNs.[56,73,74]

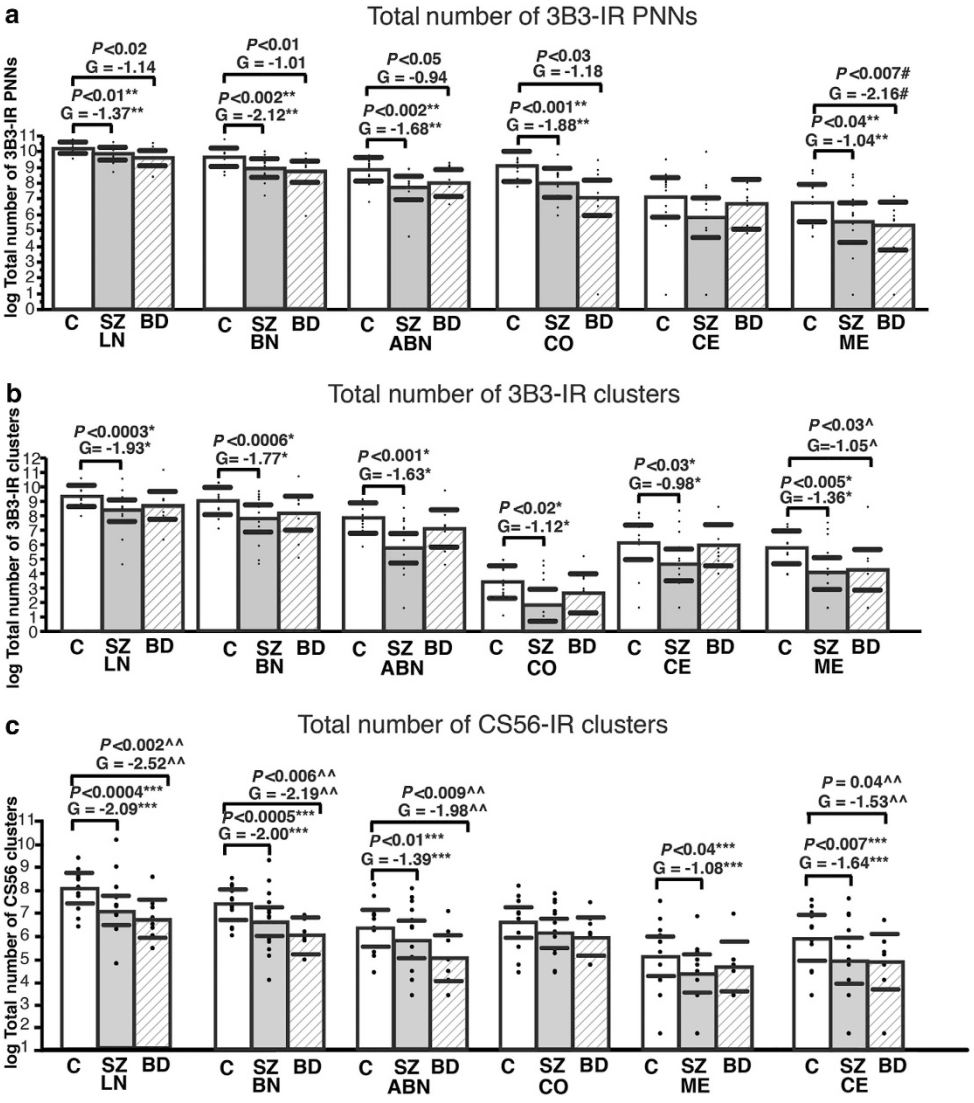

Figure 5. CS-6-IR PNNs and glial clusters are decreased in subjects with SZ and BD. (**a**) Total numbers of 3B3-IR PNNs were significantly decreased in LN, BN, ABN, ME and CO of SZ and BD subjects. (**b**) Total numbers of 3B3-IR glial cell clusters were significantly decreased in the LN, BN, AB and ME nuclei of SZ subjects. Decreases of 3B3-IR glial cell clusters in BD were restricted to ME. (**c**) Total numbers of CS56-IR glial cell clusters were significantly decreased in the LN, BN, AB and CE nuclei of SZ and BD subjects, whereas decreases in ME were only detected in SZ subjects. Scatterplots show the mean (histogram) and 95% confidence intervals (black lines). Significance values derived from stepwise linear regression models. *Adjusted for effects of age and cause of death. ^Adjusted for effects of sex and brain weight. **Adjusted for effects of cause of death, PMI and VPA. ^^Adjusted for effects of sex and CPZ lifetime in grams. #Adjusted for effect of age and brain weight. ***Adjusted for effect of exposure to SSRIs. #Adjusted for effects of age and brain weight. ABN, accessory basal nucleus; BD, bipolar disorder; BN, basal nucleus; CE, central nucleus; CO, cortical nucleus; CPZ, chlorpromazine; CS, chondroitin sulfate; IR, immunoreactivity; LN, lateral nucleus; ME, medial nucleus; PMI, postmortem time interval; PNN, perineuronal net; SSRI, selective serotonin reuptake inhibitor; SZ, schizophrenia; VPA, valproic acid.

This antibody labels a distinct glycosylated form of the aggrecan core protein, whereas other glycosylated forms may be only partially recognized.[56,75] Thus, our results on aggrecan may be specific to the form recognized by cat-301. This consideration may, at least in part, explain the discrepancy between aggrecan mRNA and protein detected in this study (see Supplementary Materials). Compensatory mechanisms leading to increased mRNA expression in response to decreased protein availability may also account for this discrepancy, as observed in other molecular systems in schizophrenia.[76,77]

Our results on aggrecan and CS-6, and previous findings using WFA, are consistent with regard to PNNs, but not with regard to glial cells.[3] Although the specific binding site for WFA is known,[58] no data are available regarding which CSPGs and sulfation patterns WFA detects. Our results show that 3B3 and aggrecan only partially colocalize with WFA in PNNs, and virtually not at all in glia (Supplementary Figures 1,2). Together, these findings indicate that WFA may not detect CS-6 sulfation patterns, at least not those recognized by 3B3 and CS56, and may label only some forms of aggrecan (see below).[45] The implication is that glial cells labeled by aggrecan (cat-301), 3B3 and CS56 do not express CSPGs labeled by WFA. Similarly, discrepancies in the patterns of 3B3, CS56 and aggrecan labeling, that is (i) 3B3- and CS56-IR glia, but not aggrecan-IR glia, express GFAP (Figure 3 and Supplementary Figure 2) and (ii) 3B3 and aggrecan label both PNNs and glia whereas CS56 only labels glia, suggest that each of these antibodies preferentially recognizes distinct CSPG/CS sulfation patterns.

Table 1. Summary of results

Dx	*Nucleus*	*Aggrecan*		*3B3*		*CS56*	*WFA*	
		Glia (%)	*PNNs (%)*	*Glia (%)*	*PNNs (%)*	*Glia (%)*	*Glia (%)*	*PNNs (%)*
SZ	LN	⇓ **−42.9**	⇓ **−48.6**	⇓ **−38.4**	⇓ **−30.1**	⇓ **−50.5**	⇑**794.4**	⇓ **−61.8**
	BN	⇓ **−37.9**	−27.6	⇓ **−33.7**	⇓ **−38.5**	⇓ **−37.5**	⇑**1162.0**	−37.7
	AB	⇓ **−45.1**	−25.3	⇓ **−56.7**	⇓ **−49.9**	⇓ **−13.0**	⇑**990.9**	36.4
	CO	0.3	−2.2	⇓ **−24.4**	⇓ **−48.1**	−8.1	⇑**418.9**	38.0
	ME	−11.6	NA	⇓ **−32.0**	−28.9	−22.7	NA	NA
	CE	⇓ **−63.4**	NA	−31.9	−8.4	⇓* **63.3**	NA	NA
BD	LN	114.5	−8.5	−5.9	⇓ **−35.4**	⇓ **−65.0**	⇑**112.2**	−39.2
	BN	88.4	13.2	15.5	⇓ **−32.0**	⇓ **−74.8**	337.5	−18.7
	AB	52.6	⇓ **−34.8**	−4.4	⇓ **−42.4**	⇓ **−37.1**	103.8	−23.8
	CO	248.3	0.2	20.0	⇓ **−53.2**	−32.5	77.9	13.8
	ME	318.3	NA	13.4	⇓ **−72.9**	−66.5	NA	NA
	CE	17.8	NA	13.8	−58.7	⇓ **−39.9**	NA	NA

Abbreviations: ABN, accessory basal nucleus; BD, bipolar disorder; BN, basal nucleus; CE, central nucleus; CO, cortical nucleus; Dx, diagnosis; LN, lateral nucleus; ME, medial nucleus; NA, not available; PNN, perineuronal net; SZ, schizophrenia. Percent differences for numerical densities in disease groups with respect to the controls. Bold values and arrows indicate statistically significant changes (analysis of covariance (ANCOVA) on log-transformed values; see also Supplementary Tables 4–6). Note that percent changes included in this Table were calculated on raw values (before log transformation), and do not reflect effects of covariates included in ANCOVA models (see Results and Supplementary Tables 4–6), thus explaining some discrepancies. For instance, ANCOVA analysis for CS56-IR glial cells in the CE of subjects with SZ shows a significant decrease once exposure to SSRI is included in the model (see Results and Supplementary Table 6; marked in this Table with ⇓*); however, if SSRI exposure is not taken into account, the numerical density of CS56-IR glial cells in the CE of SZ appears to be increased (that is, 63.3%).

Decreases of PNN in SZ and BD

In subjects with SZ, robust decreases of aggrecan- and 3B3-IR PNNs, together with marked decreases of WFA-positive PNNs previously reported,[3] strongly indicate a widespread PNN pathology. Notably, the subject cohorts used for aggrecan (in this study) and for WFA,[3] overlapped to a great extent. In the LN, where these three markers, at least in part, colocalize in PNNs, our findings suggest that PNNs may be lost or at least lack several key elements. Reports that aggrecan knockout results in loss of WFA-positive PNNs[45,46] support this possibility. In the other amygdala nuclei tested, where the large majority of PNNs detected were labeled with 3B3, but not aggrecan or WFA, a similar conclusion may be premature. However, our results do show a marked disruption of PNNs containing CS-6 positive CSPGs. Taken together, these results indicate that PNN abnormalities in the amygdala of subjects with SZ are widespread, involving the LN as well as the BN, ABN, CO and ME, and thus a range of neuronal populations broader than previously thought.

In subjects with BD, marked reductions of 3B3-IR PNNs in LN, BN, ABN, CO and ME were accompanied by more modest decreases of aggrecan-IR PNNs in the LN and ABN. These findings show, to our knowledge for the first time, a disruption of PNNs in subjects with BD. PNN decreases in this disorder were not detected using WFA.[3] Thus, CS-6 expression in PNNs in BD subjects may be decreased in the otherwise normal WFA-positive PNNs, or may reflect loss of a subset of PNNs not detectable with WFA.

Together, our findings show PNN loss/disruption in the amygdala of subjects with SZ and, perhaps to a lesser extent, BD. What may be the potential causes and consequences of the observed PNN pathology? PNNs are formed during late postnatal development,[4,26] a time period coinciding with the typical onset of psychoses. Their maturation occurs in an experience-dependent manner, requiring (i) neuronal activation through glutamatergic excitation,[78] (ii) availability of key PNN components, such as specific CSPGs, link proteins and tenascin R, (iii) expression on neurons of ECM surface receptors[79,80] and (iv) transcription factors inducing neuronal maturation.[25,38] Given that PNN numbers in SZ and BD did not correlate with duration of the illness or age at onset of the disorder, it is plausible that PNN decreases may already be present during the early phases of illness. Abnormal glutamatergic transmission, polymorphisms of genes encoding for some of their components and altered CSPG expression in glial cells may, independently or in conjunction, cause defective PNN maturation.[3,5–7,59] In addition, genome-wide association studies show that some of the proteases involved in ECM remodeling, such as MMP16, are encoded by genes strongly associated with SZ.[81] Thus, it is possible that altered ECM metabolism linked to genetic vulnerabilities may, at least in part, contribute to PNN abnormalities in SZ.

PNN maturation during late postnatal development contributes to the closure of critical periods of development, stabilizing successful synaptic connectivity and instating a restricted mode of synaptic plasticity characteristic of adulthood.[4,23,82–84] In adulthood, mature PNNs regulate synaptic functions representing the fourth element of what has been termed the 'tetrapartite' synapse.[85,86] PNNs control the lateral mobility of cell surface molecules including glutamatergic receptors, thus regulating their availability on the postsynaptic membrane specialization, modulate L-type voltage-dependent calcium channels and voltage-gated potassium channels and affect the local concentration of calcium ions.[30,31,87,88] Relevant to the present results, the role of CSPGs in these functions depends, at least in part, on their sulfation pattern; for instance CS-6 and CS-4 impact voltage-dependent calcium channels in distinct ways.[89] Overall, these functions underlie the role of the adult ECM to neuronal excitability, receptor desensitization, long-term potentiation and long-term depression.[59,87,88,90–93] A disruption of PNNs may thus contribute to altered glutamatergic transmission, synaptic connectivity and plasticity in SZ and BD. In particular, in the amygdala, the process of PNN maturation is necessary to transition from a juvenile form of plasticity, during which fear conditioning can be fully erased by extinction, to an adult form of plasticity, drastically weakening the effects of extinction on fear conditioning.[82] Our findings suggest that PNN abnormalities may impact on emotion processing and plasticity in major psychoses, potentially contributing to a disruption of fear learning reported in subjects with SZ.[94] In the LN, these changes may directly affect fear conditioning, whereas changes in the BN may impact on hippocampal context learning, and involvement of the CE, ME and ABN suggests direct effects on the bed nucleus of the stria terminalis, speculatively impacting on sustained fear mechanisms.[95–98]

Aggrecan- and CS-6 (3B3 and CS56)-IR glia: decreases in SZ and BD

We have previously shown robust increases of WFA-positive glial cells in the amygdala of subjects with SZ, but not BD.[3] As virtually all WFA-positive glial cells were found to express GFAP, and numbers of GFAP-IR cells in the same SZ subjects were normal, the observed changes are interpreted as increased CSPG expression. These findings are not easily reconciled with sharp reductions of WFA-positive PNNs, because glial cells represent a main source of CSPGs and other PNN components.[35,37,99] The present results help shed light on this apparent contradiction. We show that each of several glial subpopulations expresses a distinct array of CSPGs (see Supplementary Materials). Therefore, increased expression of WFA-labeled CSPGs in a subpopulation of GFAP-IR glial cells may coexist with abnormalities in other, distinct, glial populations in which CSPGs, including aggrecan and CS-6 sulfated CSPGs, are instead decreased. In turn, CSPG decreases in these cells may contribute to PNN reductions.

We report, for the first time, the presence of glial/CSPG clusters in the human amygdala, and their decreases in subjects with SZ and BD. These clusters were shown in rodents to surround a small number of neurons and regulate glutamatergic transmission.[70,100,101] This possibility is in line with growing evidence indicating that astrocytes form microdomains modulating glutamatergic synapses and extrasynaptic glutamate receptors, and that CSPGs (cell surface bound and as part of ECM) control (i) lateral diffusion of cell surface receptors, (ii) the extrasynaptic diffusion of negatively charged transmitters such as glutamate and (iii) the expression of glial transmitter transporters.[23,87,88,102–104] Speculatively, the distinctive cellular and molecular composition of glial/CSPG clusters may underlie their role as specialized islands, perhaps representing glial/CSPG 'macrodomains', differentially regulating neuronal activity and glutamatergic neurotransmission in particular. Glial/CSPG cluster abnormalities may thus represent a contributing factor to dysregulated glutamatergic transmission, and more broadly to neuron/glia interactions, in major psychoses.[15,22,105,106]

CONCLUSIONS

Our results show aggrecan and CS-6 sulfation abnormalities in PNNs and glia within the amygdala of SZ and BD subjects. These findings indicate that CSPG abnormalities are widespread within the amygdala, and affect distinct neuronal and glial cell populations. Notably, differences between the two disorders were observed. In SZ, reductions of aggrecan and 3B3-IR PNNs in LN, together with previously reported decreases of WFA-positive PNNs in the same nucleus, suggest PNN loss. In BD, decreased aggrecan and 3B3-IR PNNs in the absence of similar changes detected by WFA labeling suggests anomalous PNN composition. Decreases of glial cells expressing CS-6 in both SZ and BD indicate that CS-6 sulfation on these cells may differentially contribute to the changes in PNNs observed in these disorders, and may impact glutamate reuptake and neurite outgrowth. In SZ and BD, CSPG abnormalities may critically contribute to a disruption of developmental and adult neuronal functions such as synaptic plasticity, glutamate signaling and firing patterns. Speculatively, a disruption of PNNs in the amygdala may lead to unstable synaptic connectivity and altered neuronal activity that may destabilize salience encoding emotion-driven learning.

CONFLICT OF INTEREST

The authors declare no conflict of interest.

ACKNOWLEDGMENTS

We thank NIH for funding (R01MH091348 to SB), Kai C Sonntag, MD, PhD, for providing technical advice regarding quantitative PCR with reverse transcription processing and data analysis, Jason J Han, PhD, for technical advice regarding confocal microscopy, and the Harvard Brain Tissue Resource Center directed by Francine Benes, MD, PhD, for providing the brain tissue samples used in this study.

REFERENCES

1 Pantazopoulos H, Boyer-Boiteau A, Holbrook EH, Jang W, Hahn CG, Arnold SE *et al.* Proteoglycan abnormalities in olfactory epithelium tissue from subjects diagnosed with schizophrenia. *Schizophr Res* 2013; **150**: 366–372.
2 Berretta S. Extracellular matrix abnormalities in schizophrenia. *Neuropharmacology* 2012; **62**: 1584–1597.
3 Pantazopoulos H, Woo T-UW, Lim MP, Lange N, Berretta S. Extracellular matrix-glial abnormalities in the amygdala and entorhinal cortex of subjects diagnosed with schizophrenia. *Arch Gen Psychiatry* 2010; **67**: 155–166.
4 Mauney SA, Athanas KM, Pantazopoulos H, Shaskan N, Passeri E, Berretta S *et al.* Developmental pattern of perineuronal nets in the human prefrontal cortex and their deficit in schizophrenia. *Biol Psychiatry* 2013; **74**: 427–435.
5 Buxbaum JD, Georgieva L, Young JJ, Plescia C, Kajiwara Y, Jiang Y *et al.* Molecular dissection of NRG1-ERBB4 signaling implicates PTPRZ1 as a potential schizophrenia susceptibility gene. *Mol Psychiatry* 2008; **13**: 162–172.
6 Muhleisen TW, Mattheisen M, Strohmaier J, Degenhardt F, Priebe L, Schultz CC *et al.* Association between schizophrenia and common variation in neurocan (NCAN), a genetic risk factor for bipolar disorder. *Schizophr Res* 2012; **138**: 69–73.
7 So HC, Fong PY, Chen RY, Hui TC, Ng MY, Cherny SS *et al.* Identification of neuroglycan C and interacting partners as potential susceptibility genes for schizophrenia in a Southern Chinese population. *Am J Med Genet B Neuropsychiatr Genet* 2010; **153B**: 103–113.
8 Cabungcal JH, Steullet P, Morishita H, Kraftsik R, Cuenod M, Hensch TK *et al.* Perineuronal nets protect fast-spiking interneurons against oxidative stress. *Proc Natl Acad Sci USA* 2013; **110**: 9130–9135.
9 Shah A, Lodge DJ. A loss of hippocampal perineuronal nets produces deficits in dopamine system function: relevance to the positive symptoms of schizophrenia. *Transl Psychiatry* 2013; **3**: e215.
10 Uhlhaas PJ, Singer W. Abnormal neural oscillations and synchrony in schizophrenia. *Nat Rev Neurosci* 2010; **11**: 100–113.
11 Spencer KM. Visual gamma oscillations in schizophrenia: implications for understanding neural circuitry abnormalities. *Clin EEG Neurosci* 2008; **39**: 65–68.
12 Lewis DA, Hashimoto T, Volk DW. Cortical inhibitory neurons and schizophrenia. *Nat Rev Neurosci* 2005; **6**: 312–324.
13 Woo TU, Miller JL, Lewis DA. Schizophrenia and the parvalbumin-containing class of cortical local circuit neurons. *Am J Psychiatry* 1997; **154**: 1013–1015.
14 Beneyto M, Kristiansen LV, Oni-Orisan A, McCullumsmith RE, Meador-Woodruff JH. Abnormal glutamate receptor expression in the medial temporal lobe in schizophrenia and mood disorders. *Neuropsychopharmacology* 2007; **32**: 1888–1902.
15 Coyle JT. The glutamatergic dysfunction hypothesis for schizophrenia. *Harv Rev Psychiatry* 1996; **3**: 241–253.
16 Harrison PJ, Lyon L, Sartorius LJ, Burnet PW, Lane TA. The group II metabotropic glutamate receptor 3 (mGluR3, mGlu3, GRM3): expression, function and involvement in schizophrenia. *J Psychopharmacol* 2008; **22**: 308–322.
17 Javitt DC. Glutamatergic theories of schizophrenia. *Isr J Psychiatry Relat Sci* 2010; **47**: 4–16.
18 Akbarian S, Kim JJ, Potkin SG, Hetrick WP, Bunney WE Jr, Jones EG. Maldistribution of interstitial neurons in prefrontal white matter of the brains of schizophrenic patients. *Arch Gen Psychiatry* 1996; **53**: 425–436.
19 Arnold SE. Neurodevelopmental abnormalities in schizophrenia: insights from neuropathology. *Dev Psychopathol* 1999; **11**: 439–456.
20 Yang Y, Fung SJ, Rothwell A, Tianmei S, Weickert CS. Increased interstitial white matter neuron density in the dorsolateral prefrontal cortex of people with schizophrenia. *Biol Psychiatry* 2011; **69**: 63–70.
21 Bernstein HG, Steiner J, Bogerts B. Glial cells in schizophrenia: pathophysiological significance and possible consequences for therapy. *Expert Rev Neurother* 2009; **9**: 1059–1071.
22 Halassa MM, Fellin T, Haydon PG. The tripartite synapse: roles for gliotransmission in health and disease. *Trends Mol Med* 2007; **13**: 54–63.
23 Frischknecht R, Gundelfinger ED. The brain's extracellular matrix and its role in synaptic plasticity. *Adv Exp Med Biol* 2012; **970**: 153–171.
24 Dityatev A, Seidenbecher CI, Schachner M. Compartmentalization from the outside: the extracellular matrix and functional microdomains in the brain. *Trends Neurosci* 2010; **33**: 503–512.
25 Maeda N, Fukazawa N, Ishii M. Chondroitin sulfate proteoglycans in neural development and plasticity. *Front Biosci* 2010; **15**: 626–644.
26 Wang D, Fawcett J. The perineuronal net and the control of CNS plasticity. *Cell Tissue Res* 2012; **349**: 147–160.

27 Bandtlow CE, Zimmermann DR. Proteoglycans in the developing brain: new conceptual insights for old proteins. *Physiol Rev* 2000; **80**: 1267–1290.
28 Curran T, D'Arcangelo G. Role of reelin in the control of brain development. *Brain Res Brain Res Rev* 1998; **26**: 285–294.
29 Zimmermann DR, Dours-Zimmermann MT. Extracellular matrix of the central nervous system: from neglect to challenge. *Histochem Cell Biol* 2008; **130**: 635–653.
30 Dityatev A, Schachner M. The extracellular matrix and synapses. *Cell Tissue Res* 2006; **326**: 647–654.
31 Dityatev A, Schachner M, Sonderegger P. The dual role of the extracellular matrix in synaptic plasticity and homeostasis. *Nat Rev Neurosci* 2010; **11**: 735–746.
32 McRae PA, Rocco MM, Kelly G, Brumberg JC, Matthews RT. Sensory deprivation alters aggrecan and perineuronal net expression in the mouse barrel cortex. *J Neurosci* 2007; **27**: 5405–5413.
33 Gati G, Morawski M, Lendvai D, Matthews RT, Jager C, Zachar G *et al.* Chondroitin sulphate proteoglycan-based perineuronal net establishment is largely activity-independent in chick visual system. *J Chem Neuroanat* 2010; **40**: 243–247.
34 Ye Q, Miao QL. Experience-dependent development of perineuronal nets and chondroitin sulfate proteoglycan receptors in mouse visual cortex. *Matrix Biol* 2013; **32**: 352–363.
35 Faissner A, Pyka M, Geissler M, Sobik T, Frischknecht R, Gundelfinger ED *et al.* Contributions of astrocytes to synapse formation and maturation—potential functions of the perisynaptic extracellular matrix. *Brain Res Rev* 2010; **63**: 26–38.
36 Klausmeyer A, Conrad R, Faissner A, Wiese S. Influence of glial-derived matrix molecules, especially chondroitin sulfates, on neurite growth and survival of cultured mouse embryonic motoneurons. *J Neurosci Res* 2011; **89**: 127–141.
37 Wiese S, Karus M, Faissner A. Astrocytes as a source for extracellular matrix molecules and cytokines. *Front Pharmacol* 2012; **3**: 120.
38 Beurdeley M, Spatazza J, Lee HH, Sugiyama S, Bernard C, Di Nardo AA *et al.* Otx2 binding to perineuronal nets persistently regulates plasticity in the mature visual cortex. *J Neurosci* 2012; **32**: 9429–9437.
39 Bruckner G, Kacza J, Grosche J. Perineuronal nets characterized by vital labelling, confocal and electron microscopy in organotypic slice cultures of rat parietal cortex and hippocampus. *J Mol Histol* 2004; **35**: 115–122.
40 Celio MR. Perineuronal nets of extracellular matrix around parvalbumin-containing neurons of the hippocampus. *Hippocampus* 1993; **3 (Spec No)**: 55–60.
41 Pantazopoulos H, Lange N, Hassinger L, Berretta S. Subpopulations of neurons expressing parvalbumin in the human amygdala. *J Comp Neurol* 2006; **496**: 706–722.
42 Maeda N. Structural variation of chondroitin sulfate and its roles in the central nervous system. *Cent Nerv Syst Agents Med Chem* 2010; **10**: 22–31.
43 Miyata S, Komatsu Y, Yoshimura Y, Taya C, Kitagawa H. Persistent cortical plasticity by upregulation of chondroitin 6-sulfation. *Nat Neurosci* 2012; **15**: 414–422, S1-2.
44 Caterson B, Griffin J, Mahmoodian F, Sorrell JM. Monoclonal antibodies against chondroitin sulphate isomers: their use as probes for investigating proteoglycan metabolism. *Biochem Soc Trans* 1990; **18**: 820–823.
45 Giamanco KA, Morawski M, Matthews RT. Perineuronal net formation and structure in aggrecan knockout mice. *Neuroscience* 2010; **170**: 1314–1327.
46 Giamanco KA, Matthews RT. Deconstructing the perineuronal net: cellular contributions and molecular composition of the neuronal extracellular matrix. *Neuroscience* 2012; **218**: 367–384.
47 Guimaraes A, Zaremba S, Hockfield S. Molecular and morphological changes in the cat lateral geniculate nucleus and visual cortex induced by visual deprivation are revealed by monoclonal antibodies Cat-304 and Cat-301. *J Neurosci* 1990; **10**: 3014–3024.
48 Kalb RG, Hockfield S. Molecular evidence for early activity-dependent development of hamster motor neurons. *J Neurosci* 1988; **8**: 2350–2360.
49 Gu WL, Fu SL, Wang YX, Li Y, Lu HZ, Xu XM *et al.* Chondroitin sulfate proteoglycans regulate the growth, differentiation and migration of multipotent neural precursor cells through the integrin signaling pathway. *BMC Neurosci* 2009; **10**: 128.
50 Caterson B. Fell-Muir Lecture: chondroitin sulphate glycosaminoglycans: fun for some and confusion for others. *Int J Exp Pathol* 2012; **93**: 1–10.
51 Sorrell JM, Mahmoodian F, Caterson B. Immunochemical and biochemical comparisons between embryonic chick bone marrow and epiphyseal cartilage chondroitin/dermatan sulphate proteoglycans. *J Cell Sci* 1988; **91**: 81–90.
52 Deepa SS, Yamada S, Fukui S, Sugahara K. Structural determination of novel sulfated octasaccharides isolated from chondroitin sulfate of shark cartilage and their application for characterizing monoclonal antibody epitopes. *Glycobiology* 2007; **17**: 631–645.
53 Ito Y, Hikino M, Yajima Y, Mikami T, Sirko S, von Holst A *et al.* Structural characterization of the epitopes of the monoclonal antibodies 473HD, CS-56, and MO-225 specific for chondroitin sulfate D-type using the oligosaccharide library. *Glycobiology* 2005; **15**: 593–603.
54 Coggeshall RE, Lekan HA. Methods for determining number of cells and synapses: a case for more uniform standard of review. *J Comp Neurol* 1996; **364**: 6–15.
55 Gundersen HJ, Jensen EB, Kieu K, Nielsen J. The efficiency of systematic sampling in stereology--reconsidered. *J Microsc* 1999; **193**: 199–211.
56 Matthews RT, Kelly GM, Zerillo CA, Gray G, Tiemeyer M, Hockfield S. Aggrecan glycoforms contribute to the molecular heterogeneity of perineuronal nets. *J Neurosci* 2002; **22**: 7536–7547.
57 Yin ZQ, Crewther SG, Wang C, Crewther DP. Pre- and post-critical period induced reduction of Cat-301 immunoreactivity in the lateral geniculate nucleus and visual cortex of cats Y-blocked as adults or made strabismic as kittens. *Mol Vis* 2006; **12**: 858–866.
58 Kurokawa T, Tsuda M, Sugino Y. Purification and characterization of a lectin from Wistaria floribunda seeds. *J Biol Chem* 1976; **251**: 5686–5693.
59 Dityatev A, Bruckner G, Dityateva G, Grosche J, Kleene R, Schachner M. Activity-dependent formation and functions of chondroitin sulfate-rich extracellular matrix of perineuronal nets. *Dev Neurobiol* 2007; **67**: 570–588.
60 Galtrey CM, Fawcett JW. The role of chondroitin sulfate proteoglycans in regeneration and plasticity in the central nervous system. *Brain Res Rev* 2007; **54**: 1–18.
61 Hartig W, Brauer K, Bigl V, Bruckner G. Chondroitin sulfate proteoglycan-immunoreactivity of lectin-labeled perineuronal nets around parvalbumin-containing neurons. *Brain Res* 1994; **635**: 307–311.
62 Livak KJ, Schmittgen TD. Analysis of relative gene expression data using real-time quantitative PCR and the 2(-Delta Delta C(T)) Method. *Methods* 2001; **25**: 402–408.
63 Schmittgen TD, Livak KJ. Analyzing real-time PCR data by the comparative C (T) method. *Nat Protoc* 2008; **3**: 1101–1108.
64 Sims KS, Williams RS. The human amygdaloid complex: a cytologic and histochemical atlas using Nissl, myelin, acetylcholinesterase and nicotinamide adenine dinucleotide phosphate diaphorase staining. *Neuroscience* 1990; **36**: 449–472.
65 Amaral DG Price JL Pitkanen A Carmichael ST. Anatomical organization of the primate amygdaloid complex. In: Aggleton, JP (ed). *The Amygdala: Neurobiological Aspects of Emotion, Memory, and Mental Dysfunction*. Wiley-Liss: New York, NY, USA, 1992.
66 Sorvari H, Soininen H, Paljarvi L, Karkola K, Pitkanen A. Distribution of parvalbumin-immunoreactive cells and fibers in the human amygdaloid complex. *J Comp Neurol* 1995; **360**: 185–212.
67 Pantazopoulos H, Murray EA, Berretta S. Total number, distribution, and phenotype of cells expressing chondroitin sulfate proteoglycans in the normal human amygdala. *Brain Res* 2008; **1207**: 84–95.
68 Berretta S, Pantazopoulos H, Lange N. Neuron numbers and volume of the amygdala in subjects diagnosed with bipolar disorder or schizophrenia. *Biol Psychiatry* 2007; **62**: 884–893.
69 Baldessarini RJ Tarazi FI. Pharmacotherapy of psychosis and mania. In: Brunton, LL, Lazo, JS, Parker, KL (eds). *Goodman and Gilman's The Pharmacological Basis of Therapeutics*, 11th edn. McGraw-Hill Press: New York, NY, USA, 1995. 461–500.
70 Hayashi N, Tatsumi K, Okuda H, Yoshikawa M, Ishizaka S, Miyata S *et al.* DACS, novel matrix structure composed of chondroitin sulfate proteoglycan in the brain. *Biochem Biophys Res Commun* 2007; **364**: 410–415.
71 Yick LW, So KF, Cheung PT, Wu WT. Lithium chloride reinforces the regeneration-promoting effect of chondroitinase ABC on rubrospinal neurons after spinal cord injury. *J Neurotrauma* 2004; **21**: 932–943.
72 Frederick JP, Tafari AT, Wu SM, Megosh LC, Chiou ST, Irving RP *et al.* A role for a lithium-inhibited Golgi nucleotidase in skeletal development and sulfation. *Proc Natl Acad Sci USA* 2008; **105**: 11605–11612.
73 Ojima H, Kuroda M, Ohyama J, Kishi K. Two classes of cortical neurones labelled with Vicia villosa lectin in the guinea-pig. *Neuroreport* 1995; **6**: 617–620.
74 Celio MR, Blumcke I. Perineuronal nets--a specialized form of extracellular matrix in the adult nervous system. *Brain Res Brain Res Rev* 1994; **19**: 128–145.
75 Fryer HJ, Kelly GM, Molinaro L, Hockfield S. The high molecular weight Cat-301 chondroitin sulfate proteoglycan from brain is related to the large aggregating proteoglycan from cartilage, aggrecan. *J Biol Chem* 1992; **267**: 9874–9883.
76 Mirnics K, Middleton FA, Marquez A, Lewis DA, Levitt P. Molecular characterization of schizophrenia viewed by microarray analysis of gene expression in prefrontal cortex. *Neuron* 2000; **28**: 53–67.
77 Prabakaran S, Swatton JE, Ryan MM, Huffaker SJ, Huang JT, Griffin JL *et al.* Mitochondrial dysfunction in schizophrenia: evidence for compromised brain metabolism and oxidative stress. *Mol Psychiatry* 2004; **9**: 684–697, 43.
78 Dityatev A, Brückner G, Dityateva G, Grosche J, Kleene R, Schachner M. Activity-dependent formation and functions of chondroitin sulfate-rich extracellular matrix of perineuronal nets. *Dev Neurobiol* 2007; **67**: 570–588.

79 Carulli D, Rhodes KE, Fawcett JW. Upregulation of aggrecan, link protein 1, and hyaluronan synthases during formation of perineuronal nets in the rat cerebellum. *J Comp Neurol* 2007; **501**: 83–94.
80 Kwok JC, Carulli D, Fawcett JW. *In vitro* modeling of perineuronal nets: hyaluronan synthase and link protein are necessary for their formation and integrity. *J Neurochem* 2010; **114**: 1447–1459.
81 Consortium TSPG-WASG. Genome-wide association study identifies five new schizophrenia loci. *Nat Genet* 2011; **43**: 969–976.
82 Gogolla N, Caroni P, Luthi A, Herry C. Perineuronal nets protect fear memories from erasure. *Science* 2009; **325**: 1258–1261.
83 Pizzorusso T, Medini P, Berardi N, Chierzi S, Fawcett JW, Maffei L. Reactivation of ocular dominance plasticity in the adult visual cortex. *Science* 2002; **298**: 1248–1251.
84 Matsumoto-Miyai K, Sokolowska E, Zurlinden A, Gee CE, Luscher D, Hettwer S *et al.* Coincident pre- and postsynaptic activation induces dendritic filopodia via neurotrypsin-dependent agrin cleavage. *Cell* 2009; **136**: 1161–1171.
85 Dall'Oglio A, Xavier LL, Hilbig A, Ferme D, Moreira JE, Achaval M *et al.* Cellular components of the human medial amygdaloid nucleus. *J Comp Neurol* 2013; **521**: 589–611.
86 Dityatev A, Rusakov DA. Molecular signals of plasticity at the tetrapartite synapse. *Curr Opin Neurobiol* 2011; **21**: 353–359.
87 Frischknecht R, Heine M, Perrais D, Seidenbecher CI, Choquet D, Gundelfinger ED. Brain extracellular matrix affects AMPA receptor lateral mobility and short-term synaptic plasticity. *Nat Neurosci* 2009; **12**: 897–904.
88 Gundelfinger ED, Frischknecht R, Choquet D, Heine M. Converting juvenile into adult plasticity: a role for the brain's extracellular matrix. *Eur J Neurosci* 2010; **31**: 2156–2165.
89 Vigetti D, Andrini O, Clerici M, Negrini D, Passi A, Moriondo A. Chondroitin sulfates act as extracellular gating modifiers on voltage-dependent ion channels. *Cell Physiol Biochem* 2008; **22**: 137–146.
90 Kochlamazashvili G, Henneberger C, Bukalo O, Dvoretskova E, Senkov O, Lievens PM *et al.* The extracellular matrix molecule hyaluronic acid regulates hippocampal synaptic plasticity by modulating postsynaptic L-type Ca(2+) channels. *Neuron* 2010; **67**: 116–128.
91 Bukalo O, Schachner M, Dityatev A. Modification of extracellular matrix by enzymatic removal of chondroitin sulfate and by lack of tenascin-R differentially affects several forms of synaptic plasticity in the hippocampus. *Neuroscience* 2001; **104**: 359–369.
92 Zhou XH, Brakebusch C, Matthies H, Oohashi T, Hirsch E, Moser M *et al.* Neurocan is dispensable for brain development. *Mol Cell Biol.* 2001; **21**: 5970–5978.
93 Brakebusch C, Seidenbecher CI, Asztely F, Rauch U, Matthies H, Meyer H *et al.* Brevican-deficient mice display impaired hippocampal CA1 long-term potentiation but show no obvious deficits in learning and memory. *Mol Cell Biol* 2002; **22**: 7417–7427.
94 Holt DJ, Coombs G, Zeidan MA, Goff DC, Milad MR. Failure of neural responses to safety cues in schizophrenia. *Arch Gen Psychiatry* 2012; **69**: 893–903.
95 Shin JW, Geerling JC, Loewy AD. Inputs to the ventrolateral bed nucleus of the stria terminalis. *J Comp Neurol* 2008; **511**: 628–657.
96 Walker DL, Davis M. Role of the extended amygdala in short-duration versus sustained fear: a tribute to Dr. Lennart Heimer. *Brain Struct Funct* 2008; **213**: 29–42.
97 Maren S, Phan KL, Liberzon I. The contextual brain: implications for fear conditioning, extinction and psychopathology. *Nat Rev Neurosci* 2013; **14**: 417–428.
98 Li Z, Richter-Levin G. Priming stimulation of basal but not lateral amygdala affects long-term potentiation in the rat dentate gyrus *in vivo*. *Neuroscience* 2013; **246**: 13–21.
99 Siddiqui S, Horvat-Brocker A, Faissner A. The glia-derived extracellular matrix glycoprotein tenascin-C promotes embryonic and postnatal retina axon outgrowth via the alternatively spliced fibronectin type III domain TNfnD. *Neuron Glia Biol* 2008; **4**: 271–283.
100 Horii-Hayashi N, Tatsumi K, Matsusue Y, Okuda H, Okuda A, Hayashi M *et al.* Chondroitin sulfate demarcates astrocytic territories in the mammalian cerebral cortex. *Neurosci Lett* 2010; **483**: 67–72.
101 Okuda H, Tatsumi K, Morita S, Shibukawa Y, Korekane H, Horii-Hayashi N *et al.* Chondroitin sulfate proteoglycan tenascin-R regulates glutamate uptake by adult brain astrocytes. *J Biol Chem* 2014; **289**: 2620–2631.
102 Bridges R, Lutgen V, Lobner D, Baker DA. Thinking outside the cleft to understand synaptic activity: contribution of the cystine-glutamate antiporter (System xc-) to normal and pathological glutamatergic signaling. *Pharmacol Rev* 2012; **64**: 780–802.
103 Shan D, Yates S, Roberts RC, McCullumsmith RE. Update on the neurobiology of schizophrenia: a role for extracellular microdomains. *Minerva psichiatr* 2012; **53**: 233–249.
104 Ye ZC, Sontheimer H. Modulation of glial glutamate transport through cell interactions with the extracellular matrix. *Int J Dev Neurosci* 2002; **20**: 209–217.
105 Goudriaan A, de Leeuw C, Ripke S, Hultman CM, Sklar P, Sullivan PF *et al.* Specific glial functions contribute to schizophrenia susceptibility. *Schizophr Bull* 2013; **40**: 925–935.
106 Meador-Woodruff JH, Healy DJ. Glutamate receptor expression in schizophrenic brain. *Brain Res Brain Res Rev* 2000; **31**: 288–294.

Supplementary Information accompanies the paper on the Translational Psychiatry website (http://www.nature.com/tp)